A Standard Model for CRs Physics with AMS-02: mission accomplished

Istituto Nazionale di Fisica Nucleare

ALMA MATER STUDIORUM
UNIVERSITÀ DI BOLOGNA

Nicolò Masi

Explaining $Z \leq 28$ CRs physics by means of GALPROP and HelMod

- AMS-02 published data are fitted in the combined framework of GALPROP and HelMod (for Galactic and Heliosphere propagation, respectively) **with a single model**, capable of reproducing all primary and secondary spectra at the same time (*see* ApJ **840**:115 No 2, 2017; ApJ **854**:94 No 2, 2018; ApJ **858**:61 No 1, 2018; ApJ 889:167, 2020, ApJS **250** 27, 2020);
- The 28 proposed LISs fit Voyager 1, ACE, Pamela, AMS-02 (and many other experiments) and recent CALET and DAMPE data, from 10 MeV/n up to 200 TeV/n, representing a **reference model for the Collaboration** and a **forecasting tool for astroparticle and solar physics.**

MCMC Matrix Approach

M. Boschini, S. della Torre, N. Masi, I. Moskalenko, L. Quadrani, P.G. Rancoita *et al.*,
Solution Of Heliospheric Propagation: Unveiling The Local Interstellar Spectra Of Cosmic Ray Species,
The Astrophysical Journal **840**:115 No 2, 2017, arXiv:1704.06337

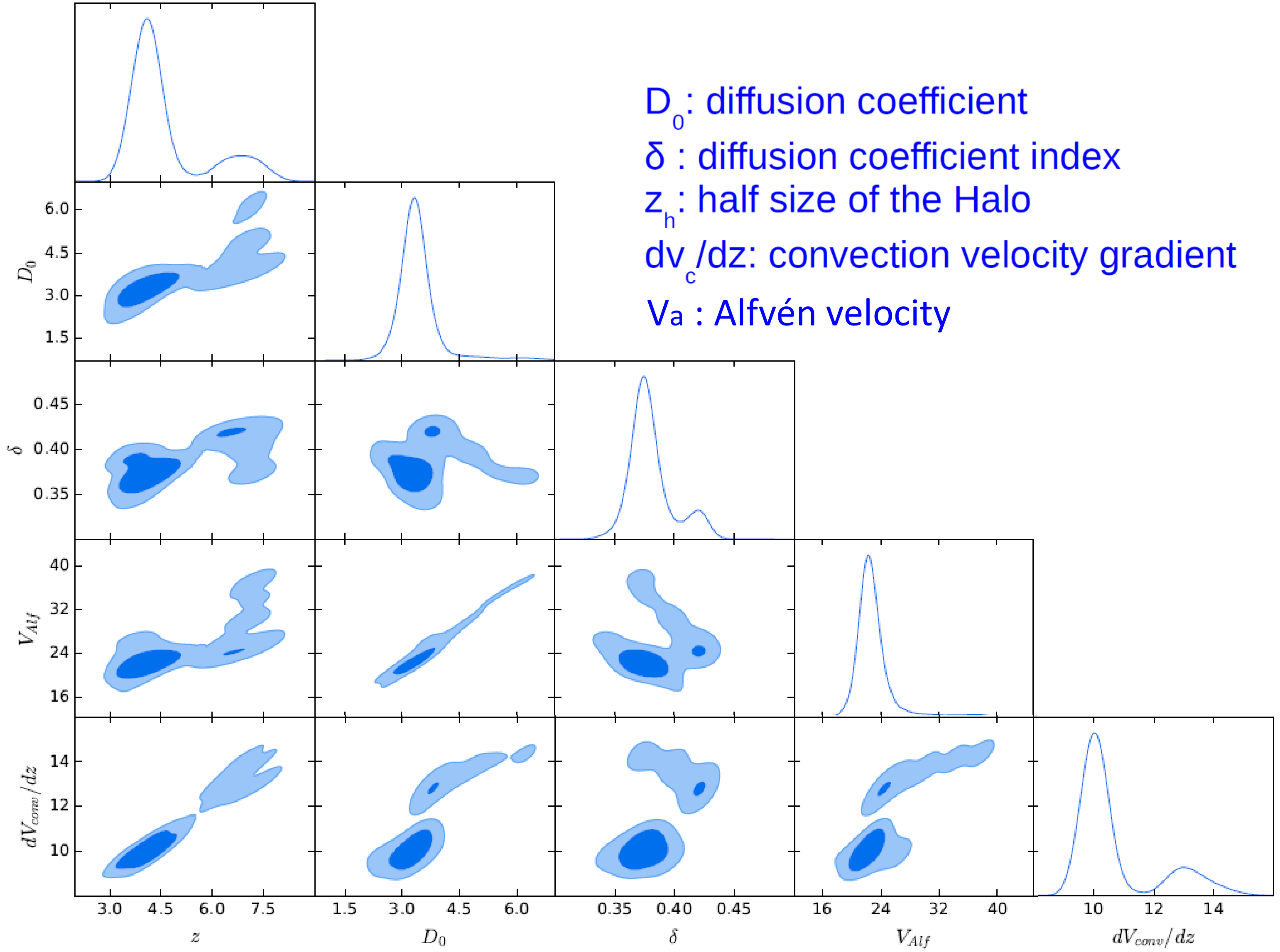

D_0: diffusion coefficient

δ : diffusion coefficient index

z_h: half size of the Halo

dv_c/dz: convection velocity gradient

Va : Alfvén velocity

1. The Monte-Carlo-Markov-Chain interface to **GALPROP v56** was **developed in Bologna** from CosRay-MC and COSMOMC package, embedding GALPROP framework into the MCMC scheme;
2. The simulations run on Ravenna pc farm;
3. The solar modulation is made using **HelMod**;
4. The experimental observables used in the MCMC scan include all primary CRs AMS-02 data and B/C ratio.

One order of magnitude of improvement for fundamental parameters uncertainties

New AMS-02 Z>8 Nuclei

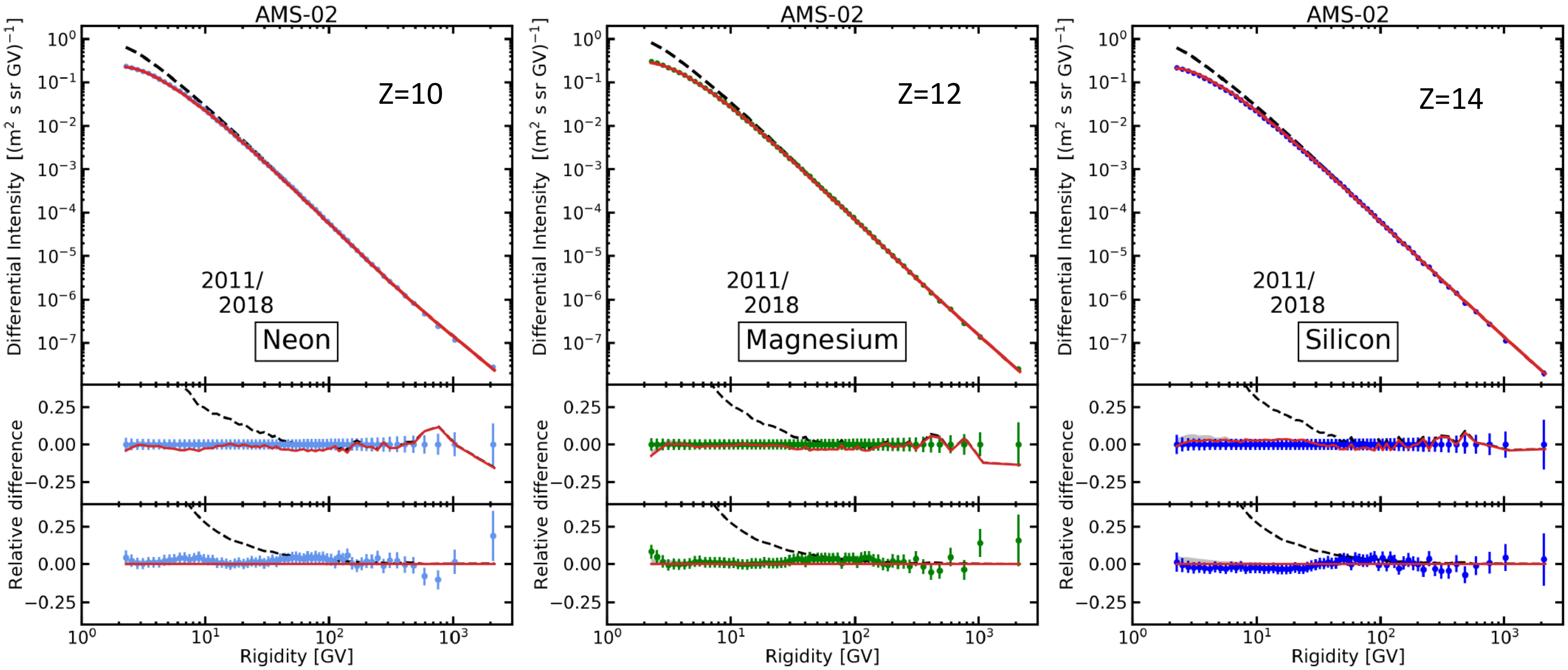

AMS-02 data from PHYSICAL REVIEW LETTERS **124**, 211102 (2020)

Updated secondary over primary ratio: B/C

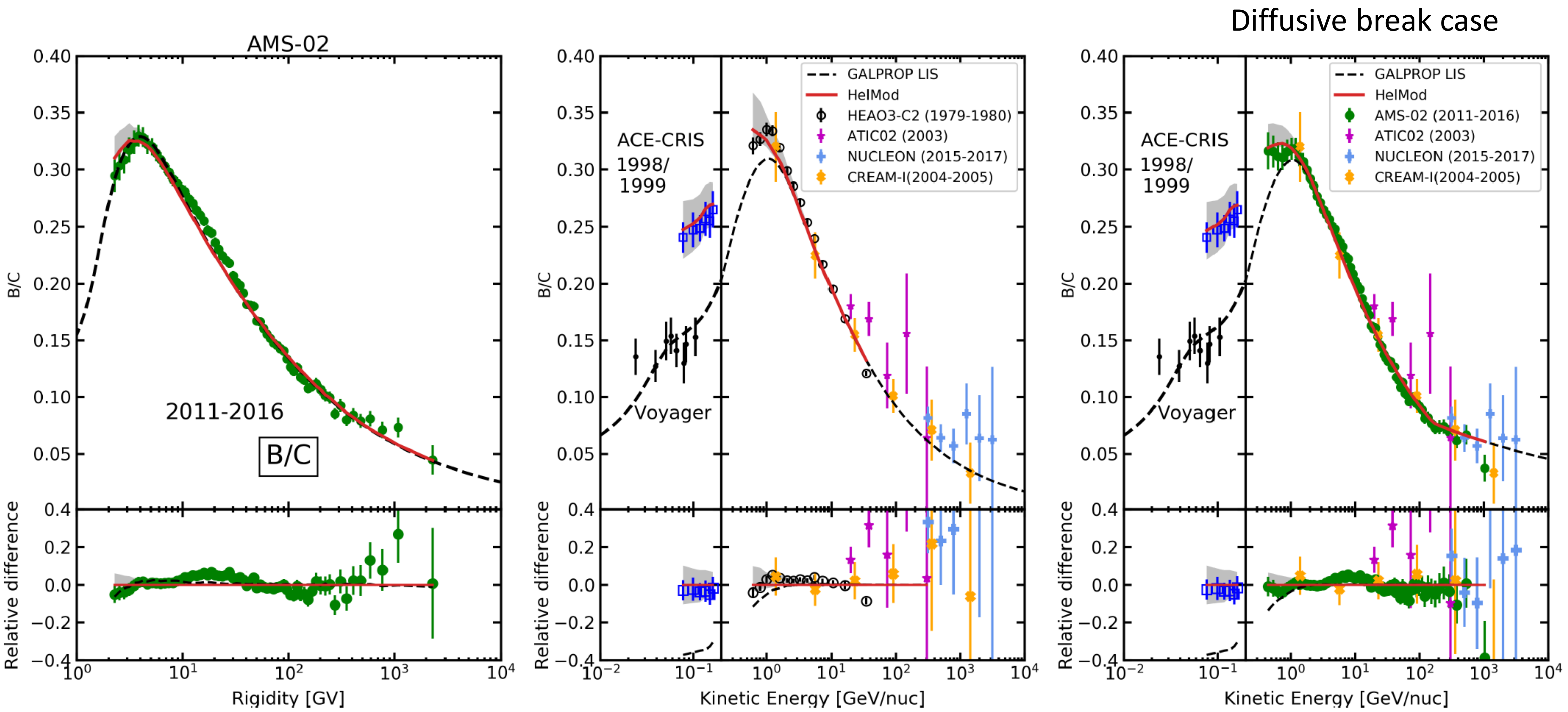

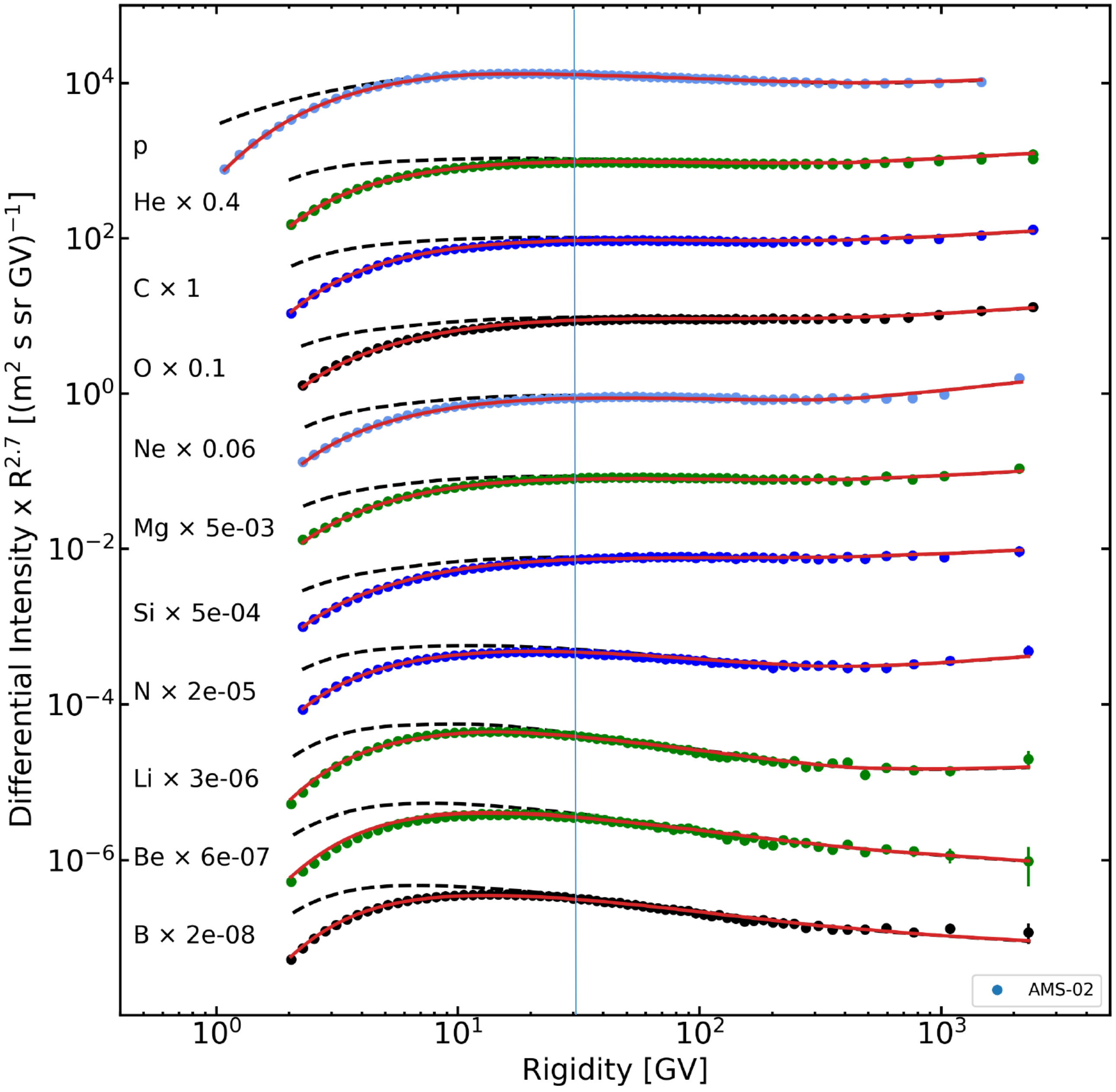

The Model confirms its prediction capability for all AMS-02 species with a single set of parameters

Primary Lithium Discovery

Primary Lithium from Novae is mandatory to explain AMS-02 measurement

the observed stellar lithium abundances indicate that some proportion of lithium is also produced in low-mass stars and nova explosions. Indeed, the alpha-capture reaction of ^{7}Be production ^{3}He$(\alpha,\gamma)^7$Be was proposed a while ago (Cameron 1955; Cameron & Fowler 1971). A subsequent decay of ^{7}Be with a half-life of 53.22 days yields ^{7}Li isotope. To ensure that produced ^{7}Li is not destroyed in subsequent nuclear reactions, ^{7}Be should be transported into cooler layers where it can decay to ^{7}Li, the so-called Cameron-Fowler mechanism.

Recent observation of blue-shifted absorption lines of partly ionized ^{7}Be in the spectrum of a classical novae V339 Del about 40-50 days after the explosion (Tajitsu et al. 2015) is the first observational evidence that the mechanism proposed in 1970s is working indeed (Hernanz 2015)

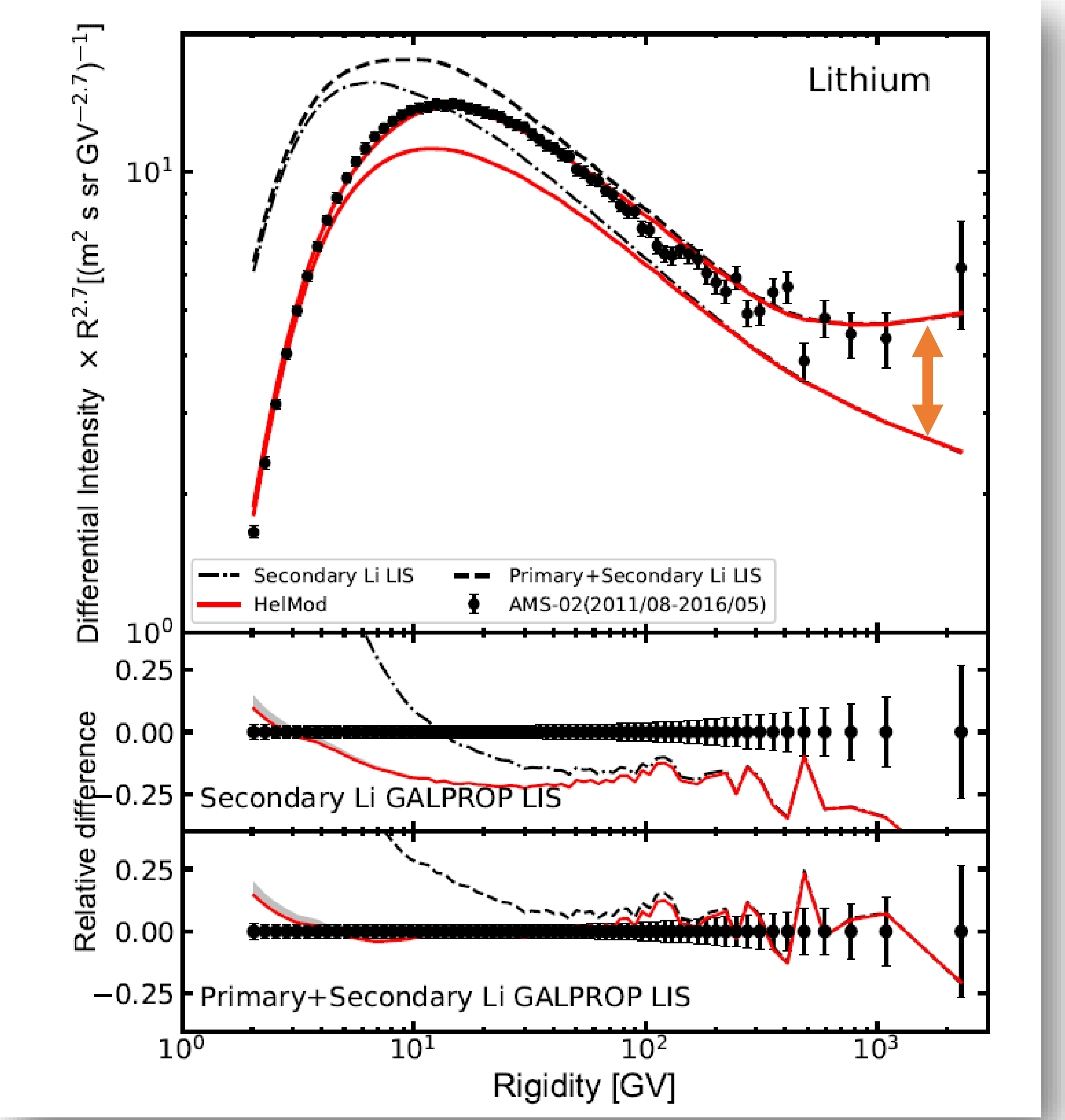

LISs validity is extended up to tens (and hundreds) GeV/n for both injection and diffusive scenarios

Injection breaks scenario

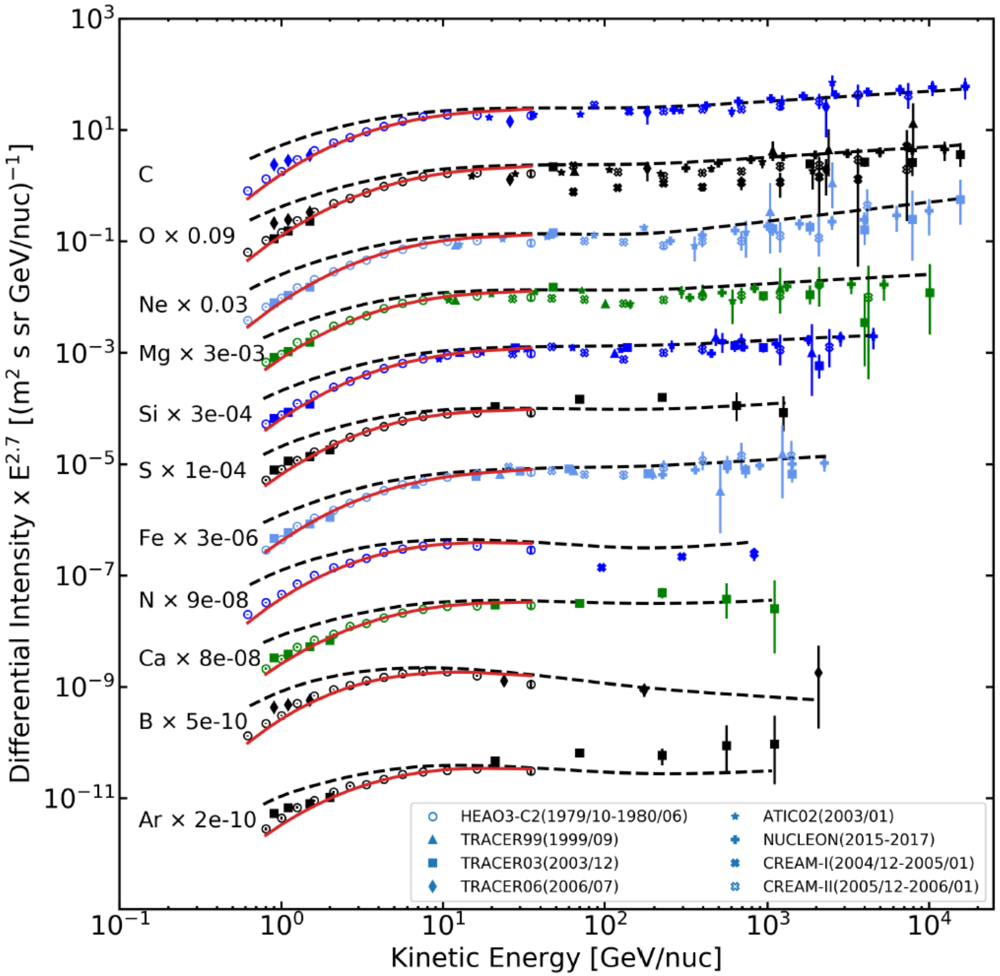

Diffusive break scenario

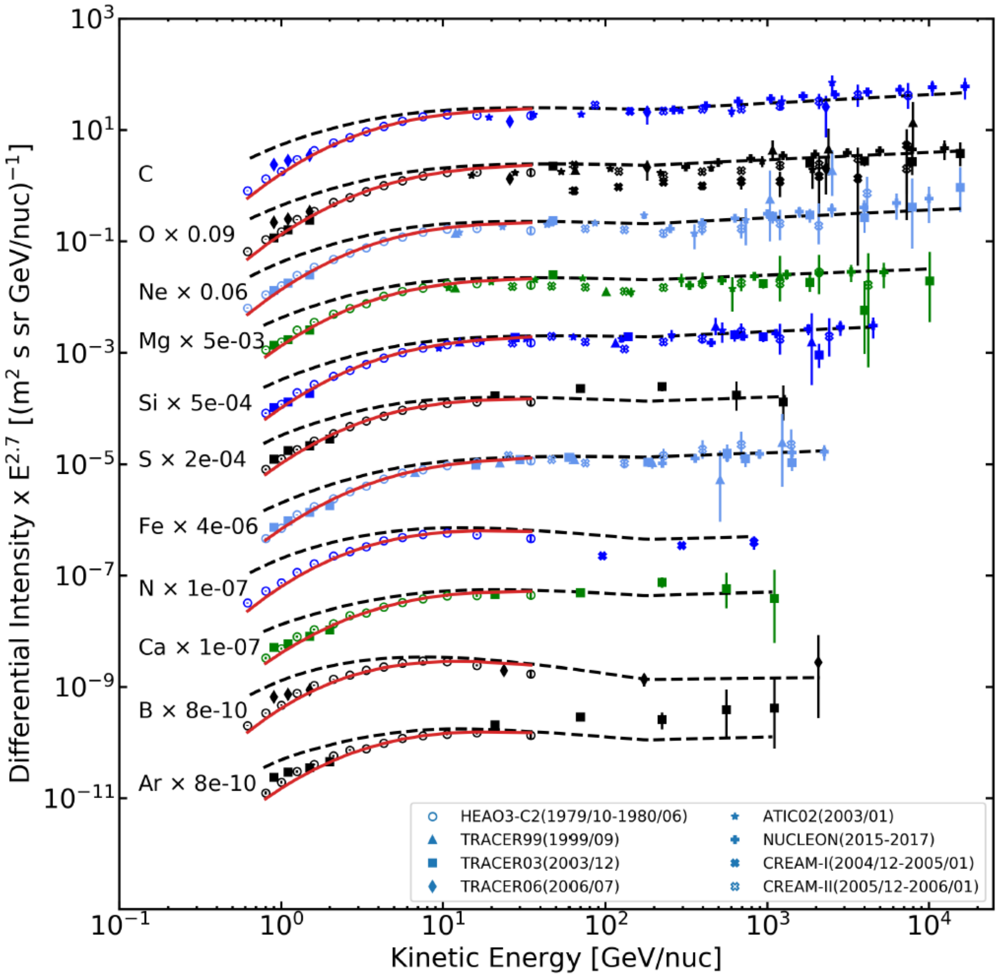

Injection versus Propagation scenarios to explain CRs hardening above 300 GV

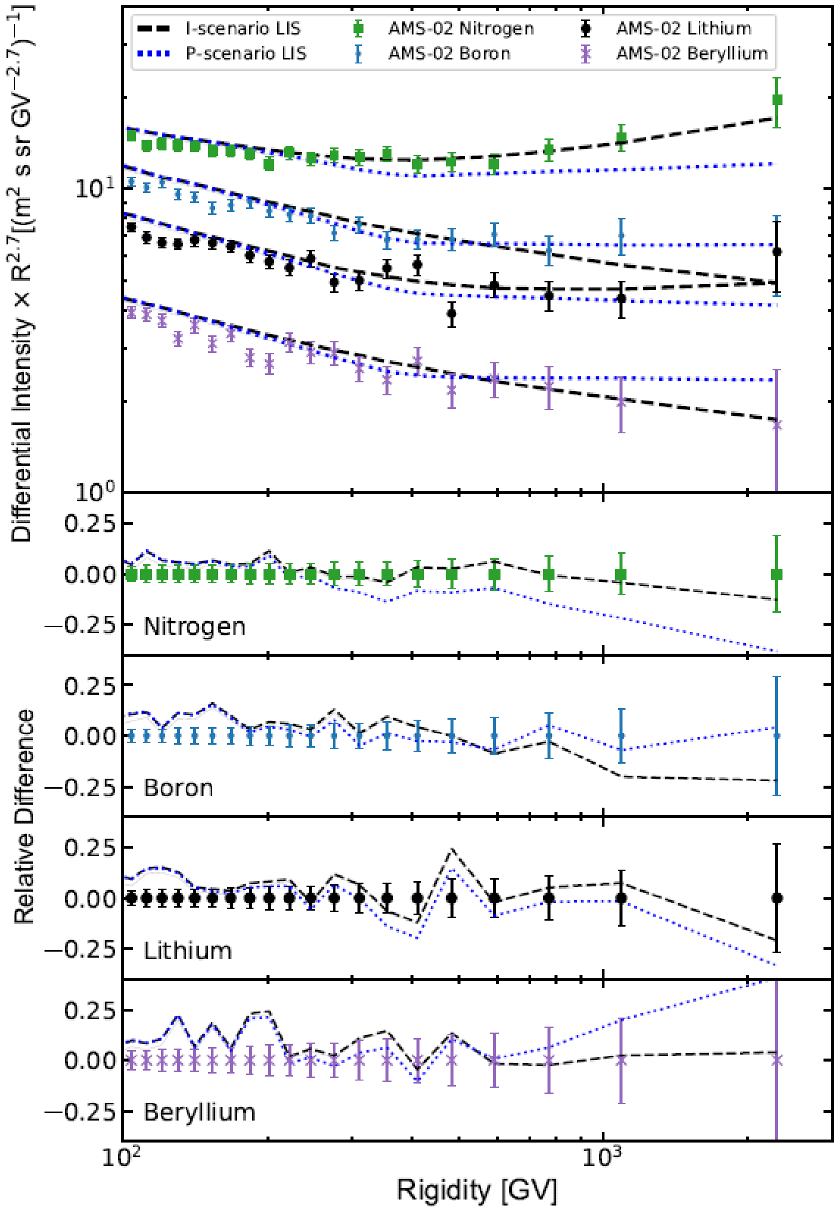

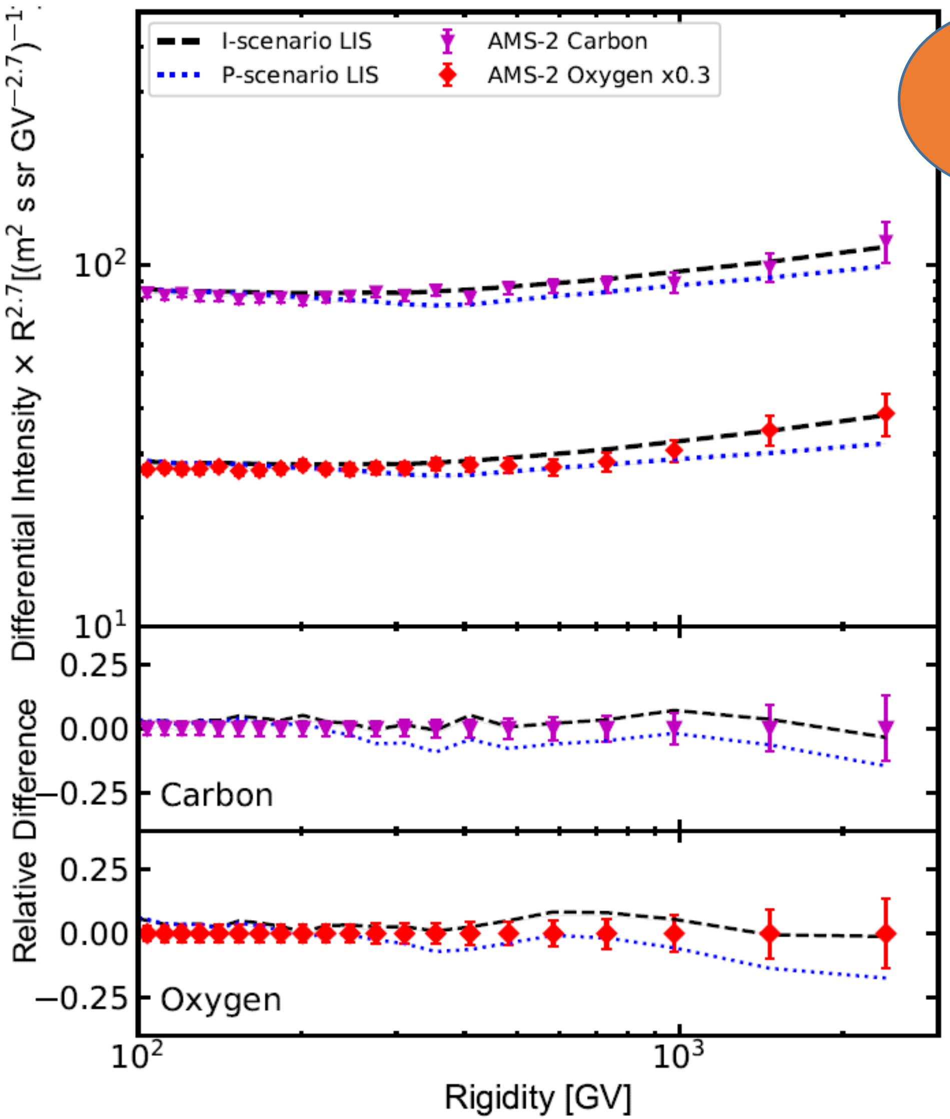

I or P?

Extension of AMS-02 based LISs for p and He with CALET and DAMPE

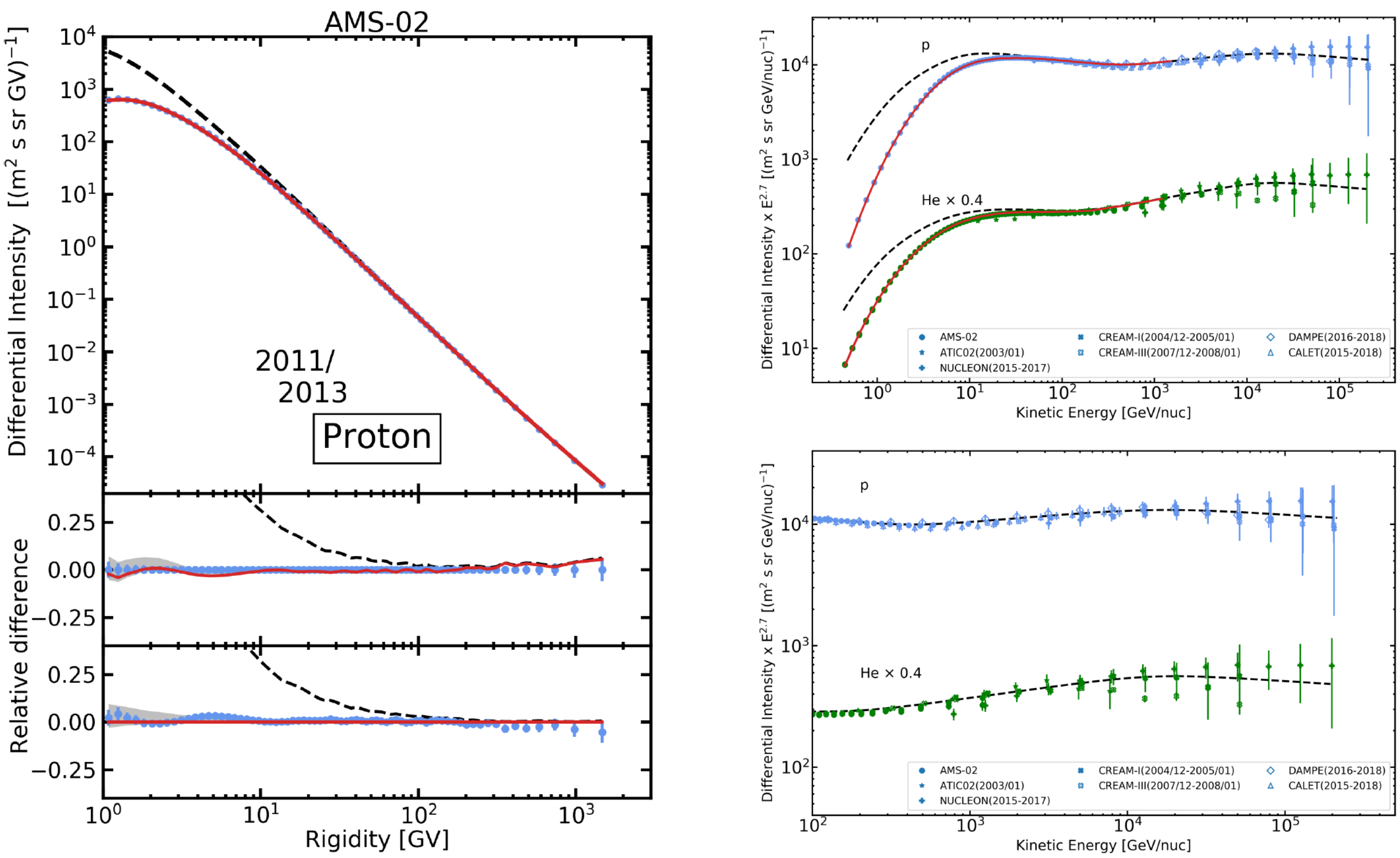

New universal behaviour with a 20 TeV/n break?

HEAO vs AMS-02 Normalization to forecast Z >14 nuclei

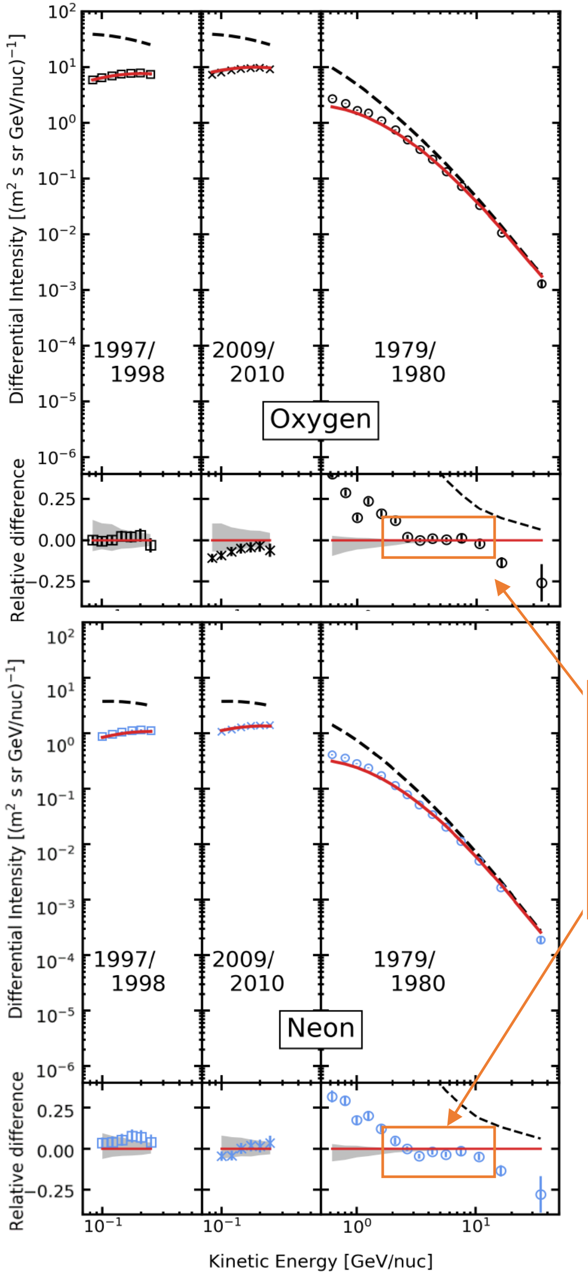

AMS-02 and HEAO normalization coincide at the % level in this region

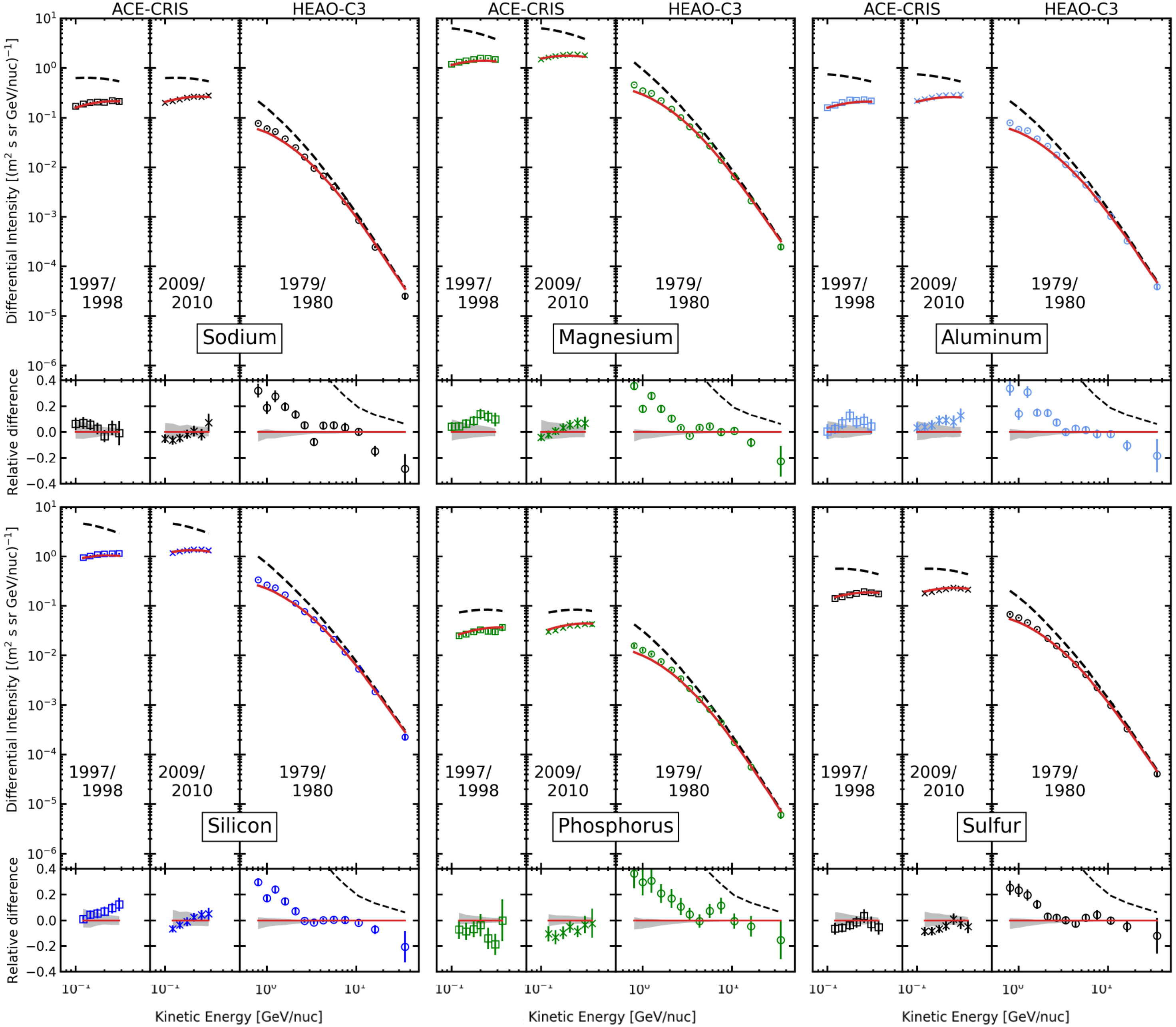

Aluminum and Sodium

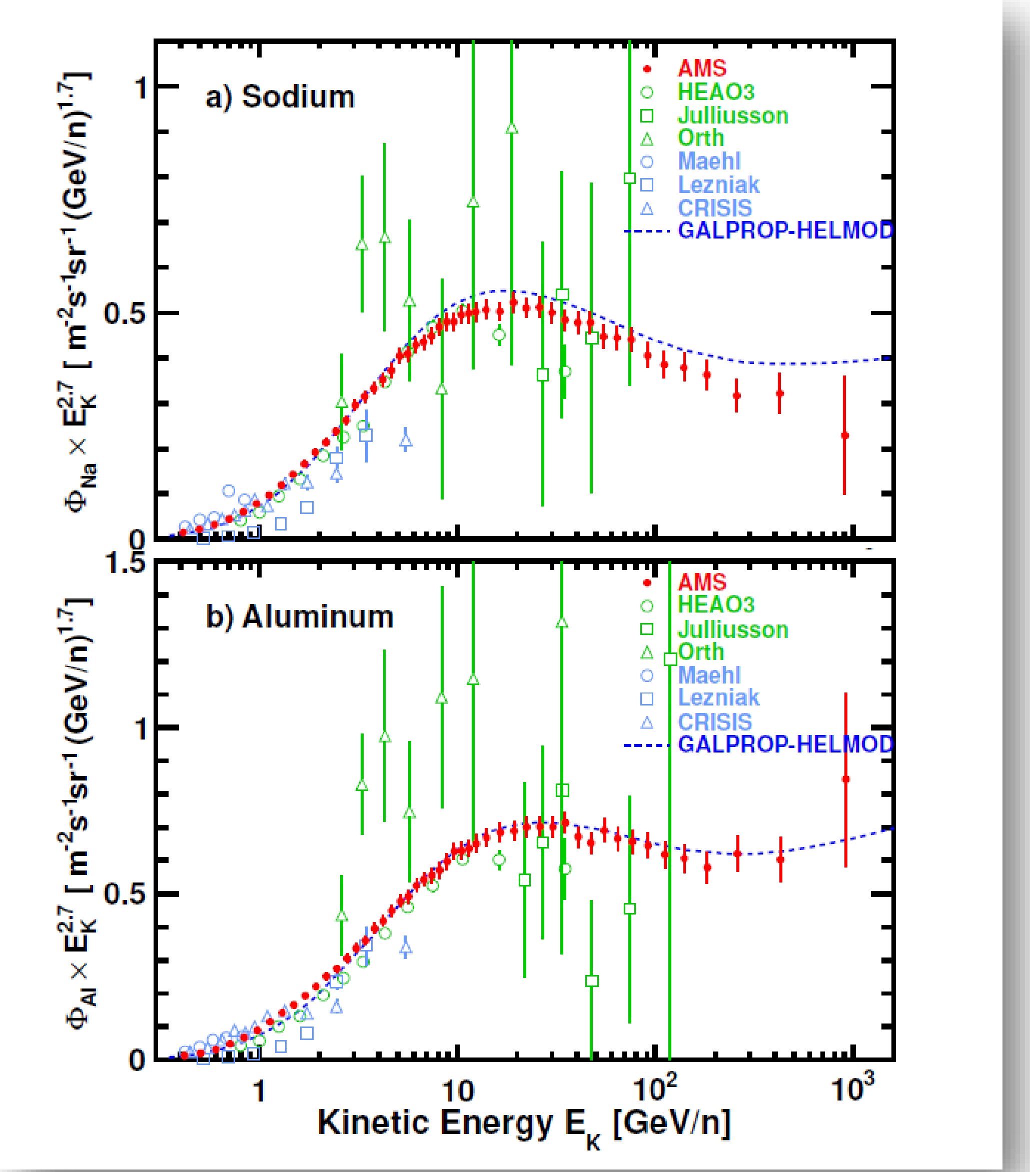

AMS-02 and HEAO normalization are very similar

Injection power laws and source abundances for Z ≤ 28 nuclei (including isotopes)

Table 2. Injection spectra of CR species

Nucleus	γ_0	R_0 (GV)	s_0	γ_1	R_1 (GV)	s_1	γ_2	R_2 (GV)	s_2	γ_3	R_3 (TV)	s_3	γ_4
$_1$H	2.24	0.95	0.29	1.70	6.97	0.22	2.44	400	0.09	2.19	16	0.09	2.37
$_2$He	2.05	1.00	0.26	1.76	7.49	0.33	2.41	340	0.13	2.12	30	0.10	2.37
${}^{7}_{3}$Li^{a}	…		…	1.10	12.0	0.16	2.72	355	0.13	1.90		…	…
$_6$C	1.00	1.10	0.19	1.98	6.54	0.31	2.43	348	0.17	2.12		…	…
${}^{14}_{7}$N	1.00	1.30	0.17	1.96	7.00	0.20	2.46	300	0.17	1.90		…	…
$_8$O	0.95	0.90	0.18	1.99	7.50	0.30	2.46	365	0.17	2.13		…	…
$_9$F	0.20	1.50	0.19	1.97	7.00	0.20	2.48	355	0.17	2.14		…	…
$_{10}$Ne	0.60	1.15	0.17	1.92	9.42	0.26	2.44	355	0.17	1.97		…	…
$_{11}$Na	0.50	0.75	0.17	1.98	7.00	0.21	2.49	355	0.17	2.14		…	…
$_{12}$Mg	0.20	0.85	0.12	1.99	7.00	0.23	2.48	355	0.17	2.15		…	…
$_{13}$Al	0.20	0.60	0.17	2.04	7.00	0.20	2.48	355	0.17	2.14		…	…
$_{14}$Si	0.20	0.85	0.17	1.97	7.00	0.26	2.47	355	0.17	2.19		…	…
$_{15}$P	0.25	1.60	0.19	1.95	7.00	0.20	2.48	355	0.17	2.14		…	…
$_{16}$S	0.80	1.30	0.17	1.96	7.00	0.20	2.49	355	0.17	2.14		…	…
$_{17}$Cl	1.10	1.50	0.17	1.98	7.20	0.20	2.53	355	0.17	2.14		…	…
$_{18}$Ar	0.20	1.30	0.17	1.96	7.00	0.20	2.46	355	0.17	2.09		…	…
$_{19}$K	0.20	1.40	0.15	1.96	7.00	0.20	2.53	355	0.17	2.14		…	…
$_{20}$Ca	0.30	1.00	0.11	2.07	7.00	0.20	2.48	355	0.17	2.14		…	…
$_{21}$Sc	0.20	1.40	0.17	1.97	7.00	0.22	2.53	355	0.17	2.14		…	…
$_{22}$Ti	1.50	0.90	0.17	1.98	7.00	0.22	2.57	355	0.17	2.14		…	…
$_{23}$V	1.10	0.80	0.17	1.98	7.00	0.22	2.53	355	0.17	2.14		…	…
$_{24}$Cr	1.70	0.65	0.17	1.99	7.00	0.20	2.48	355	0.17	2.14		…	…
$_{25}$Mn	0.20	0.85	0.10	2.08	7.00	0.20	2.48	355	0.17	2.14		…	…
$_{26}$Fe	0.27	1.04	0.18	1.99	7.00	0.20	2.51	355	0.17	2.19		…	…
$_{27}$Co	0.80	0.70	0.15	1.98	7.00	0.20	2.49	355	0.17	2.14		…	…
$_{28}$Ni	1.50	0.65	0.17	1.98	7.00	0.20	2.48	355	0.17	2.14		…	…

Table 3. Source Abundances of CR species

Nucleus	Source Abundance	Nucleus	Source Abundance	Nucleus	Source Abundance
${}^{1}_{1}$H	8.77×10^{5}	${}^{27}_{13}$Al	51.1	^{48}Ti	$<10^{-4}$
^{2}H	35	${}^{28}_{14}$Si	580	^{49}Ti	$<10^{-4}$
${}^{3}_{2}$He	$<10^{-4}$	^{29}Si	35	^{50}Ti	$<10^{-4}$
^{4}He	7.74×10^{4}	^{30}Si	24.7	${}^{50}_{23}$V	$<10^{-4}$
${}^{6}_{3}$Li	$<10^{-4}$	${}^{31}_{15}$P	5.7	^{51}V	$<10^{-4}$
^{7}Li	52	${}^{32}_{16}$S	82.1	${}^{50}_{24}$Cr	4
${}^{7}_{4}$Be	0	^{33}S	0.306	^{51}Cr	0
^{9}Be	$<10^{-4}$	^{34}S	3.42	^{52}Cr	11.1
^{10}Be	$<10^{-4}$	^{36}S	4.28×10^{-4}	^{53}Cr	3.01×10^{-3}
${}^{10}_{5}$B	1.80×10^{-4}	${}^{35}_{17}$Cl	2.5	^{54}Cr	0.5
^{11}B	7.42×10^{-4}	^{37}Cl	1.17×10^{-3}	${}^{53}_{25}$Mn	12.6
${}^{12}_{6}$C	2720	${}^{36}_{18}$Ar	11.4	^{55}Mn	2.9
^{13}C	$<10^{-4}$	^{38}Ar	0.74	${}^{54}_{26}$Fe	30.1
${}^{14}_{7}$N	207	^{40}Ar	1.74×10^{-3}	^{55}Fe	0
^{15}N	$<10^{-4}$	${}^{39}_{19}$K	1.39	^{56}Fe	515
${}^{16}_{8}$O	3510	^{40}K	2.80	^{57}Fe	17.7
^{17}O	$<10^{-4}$	^{41}K	3.34×10^{-4}	^{58}Fe	5.34
^{18}O	1.29	${}^{40}_{20}$Ca	36.1	${}^{59}_{27}$Co	1.40
${}^{19}_{9}$F	0.95	^{41}Ca	1.97	${}^{58}_{28}$Ni	22.3
${}^{20}_{10}$Ne	338	^{42}Ca	$<10^{-4}$	^{59}Ni	0
^{21}Ne	3.56×10^{-3}	^{43}Ca	$<10^{-4}$	^{60}Ni	8.99
^{22}Ne	107	^{44}Ca	$<10^{-4}$	^{61}Ni	0.599
${}^{23}_{11}$Na	24.1	^{48}Ca	0.11	^{62}Ni	1.43
${}^{24}_{12}$Mg	490	${}^{45}_{21}$Sc	1.46	^{64}Ni	0.304
^{25}Mg	70	${}^{46}_{22}$Ti	4.9	…	…
^{26}Mg	90	^{47}Ti	$<10^{-4}$	…	…

Full description of CR abundances: Source vs Propagated

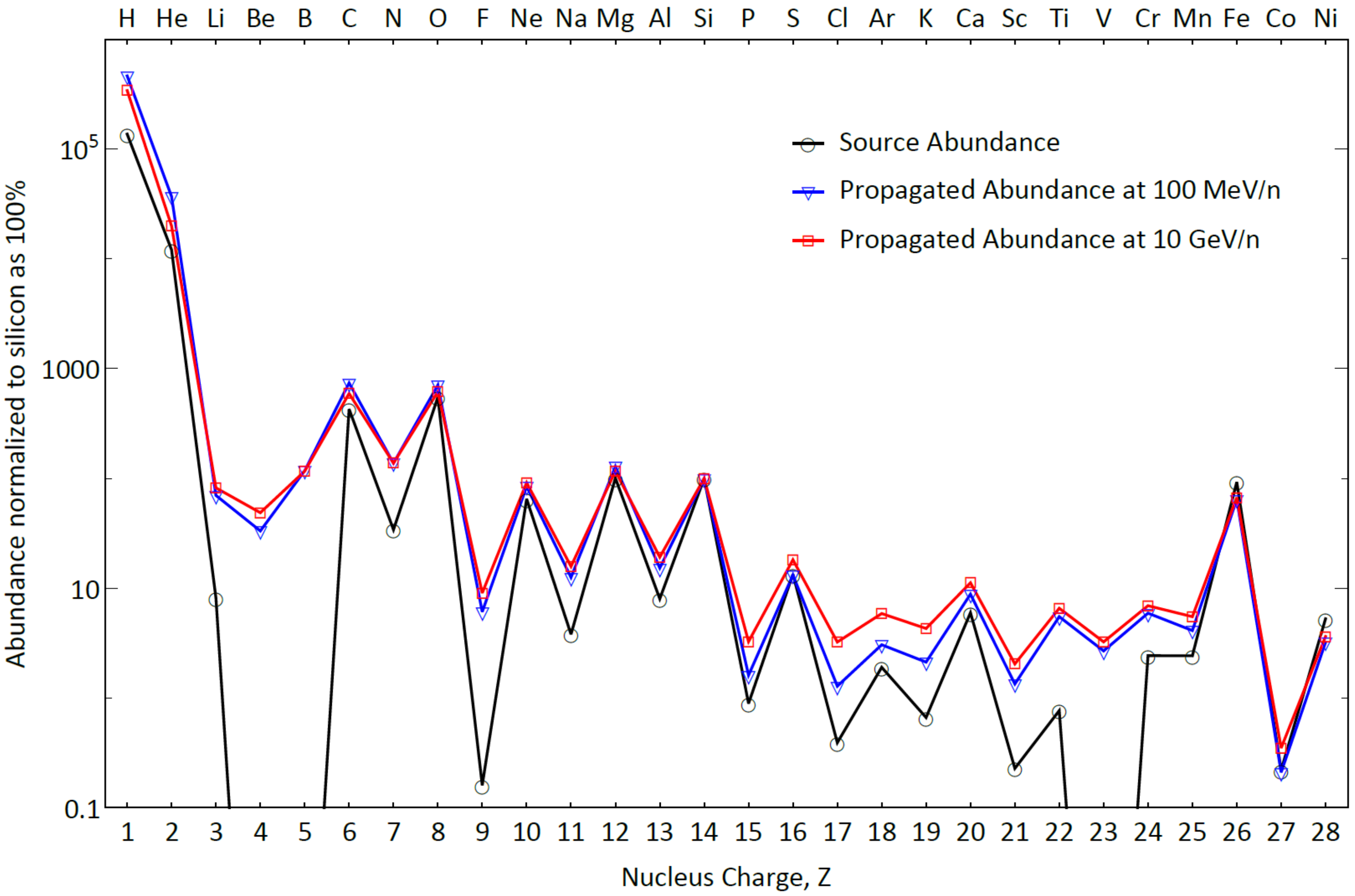

Interstellar spectra measured by Voyager-1

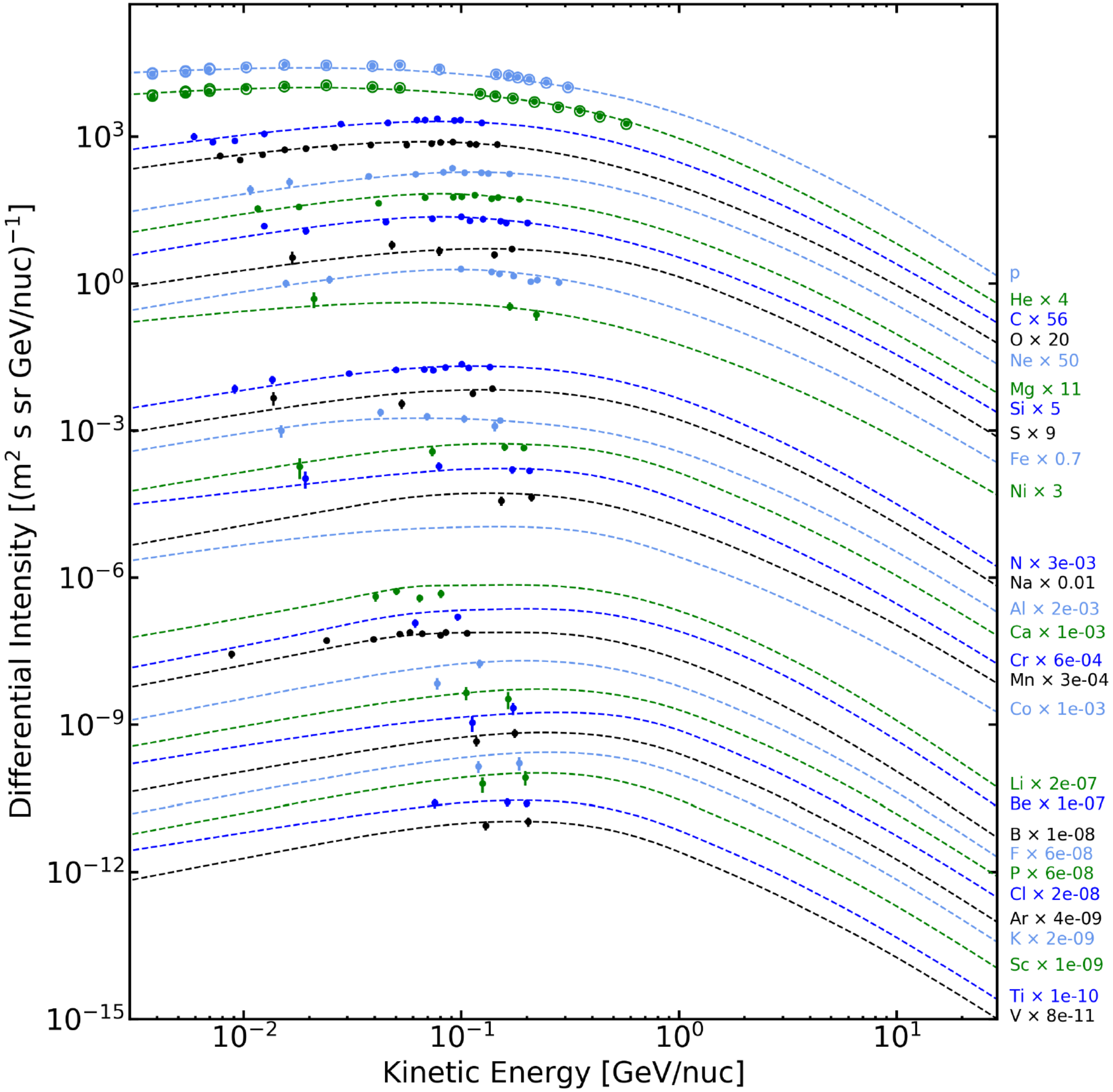

All Z ≤ 28 are well reproduced

Our website provides numerical LISs, analytical formulas and plots

Website Search

Search ...

HelMod Long Write Up

- The HelMod Model
- HelMod Heliosphere
- Heliospheric boundaries in HelMod
- Heliospheric Magnetic Field
- Diffusion Parameter
- Diffusion tensor
- Monte Carlo Integration
- Current and Historical Values of default parameters
- Interpolation Functions for Local Interstellar Spectra
- HelMod Results
- HelMod Forecasting

HelMod Web Calculators

- Mission Integrated Differential Intensity and Forecast
- Stand-Alone Module (offline)

News

Updated Offline Archives to v4.1

released 4.1 version

Related Link

- GALPROP
- Wilcox Solar Observatory
- SILSO
- OMNIWeb
- Geomagsphere
- SR-NIEL web calculator
- SR-NIEL physics handbook
- ASIF - ASI Supported Irradiation Facilities

Local Interstellar Spectra from Galprop-HelMod join effort

By exploiting experimental results, the combined effort of the physicists involved with the Galprop model for propagation in galaxy and HelMod for the propagation in heliosphere, the local interstellar spectra (LIS) for Galactic Cosmic Rays species up to Z=28 (Nickel) were derived. These spectra are available and accessible from the current webpage.

Selected LIS: 26: Iron

Some of the currently available LIS's were derived accounting for AMS-02 data published up to TV rigidity region. The exploitation of AMS-02 data allowed one to approach the procedure with high statistic data of unprecedent accuracy. Currently, the observation data at Earth on cosmic rays species from HEAO3-C2 (from october 1979 to June 1980) and AMS-02 were employed for absolute scale normalization of fluxes (see Sects. 3-3.2 in Boschini et al. 2020).

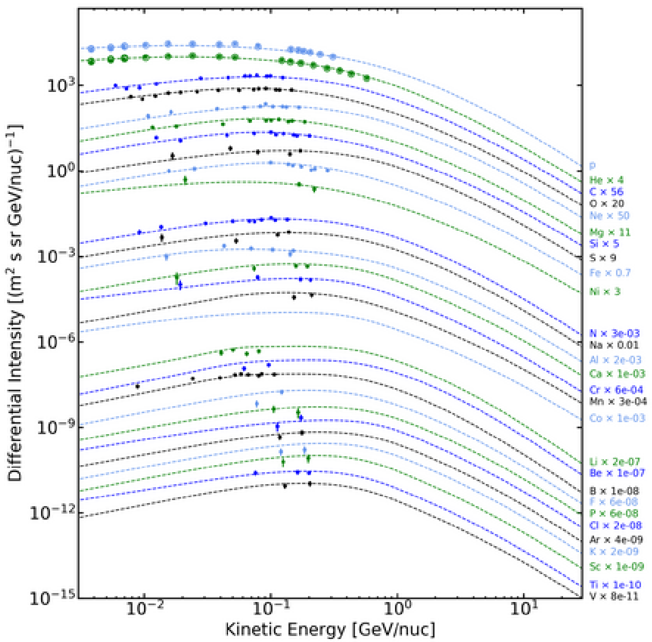

The GALPROP LIS for all CR species (dashed lines) are compared to the Voyager 1 data (filled circles, Cummings et al 2016). We also show updated Voyager 1 data for H and He (open circles) taken from September 1, 2012 to November 13, 2019. The elements are sorted by approximate amount of primary contribution: first group is mostly primary, second – with significant primary contribution, and third – mostly secondary.

LISs will be futher fine-tuned and updated on the website using incoming AMS-02 measurements

2020 Achievements - 2021 Resolutions

- ✓ All cosmic rays species with $Z \leq 28$ predicted with GALPROP plus HelMod
- ✓ General reference framework for incoming Collaboration measurements and astroparticle community
- ✓ Extension of LISs validity up to 100 TeV/n scale
- ✓ Study of high mass nuclei, abundances and possible anomalous secondaries
- ✓ Iron spectrum and its fine features (ongoing)

- ✓ High mass primary/half-primary (Na-Al-S) and secondaries (Fluorine);
- ✓ Iron/sub Iron predictions
- ✓ Isotopes physics (d, Li, Be, B…)
- ✓ Fundamental propagation questions: testing injection vs diffusive breaks scenarios, possible nearby sources and pre-knee new behaviors

Backup

Iron

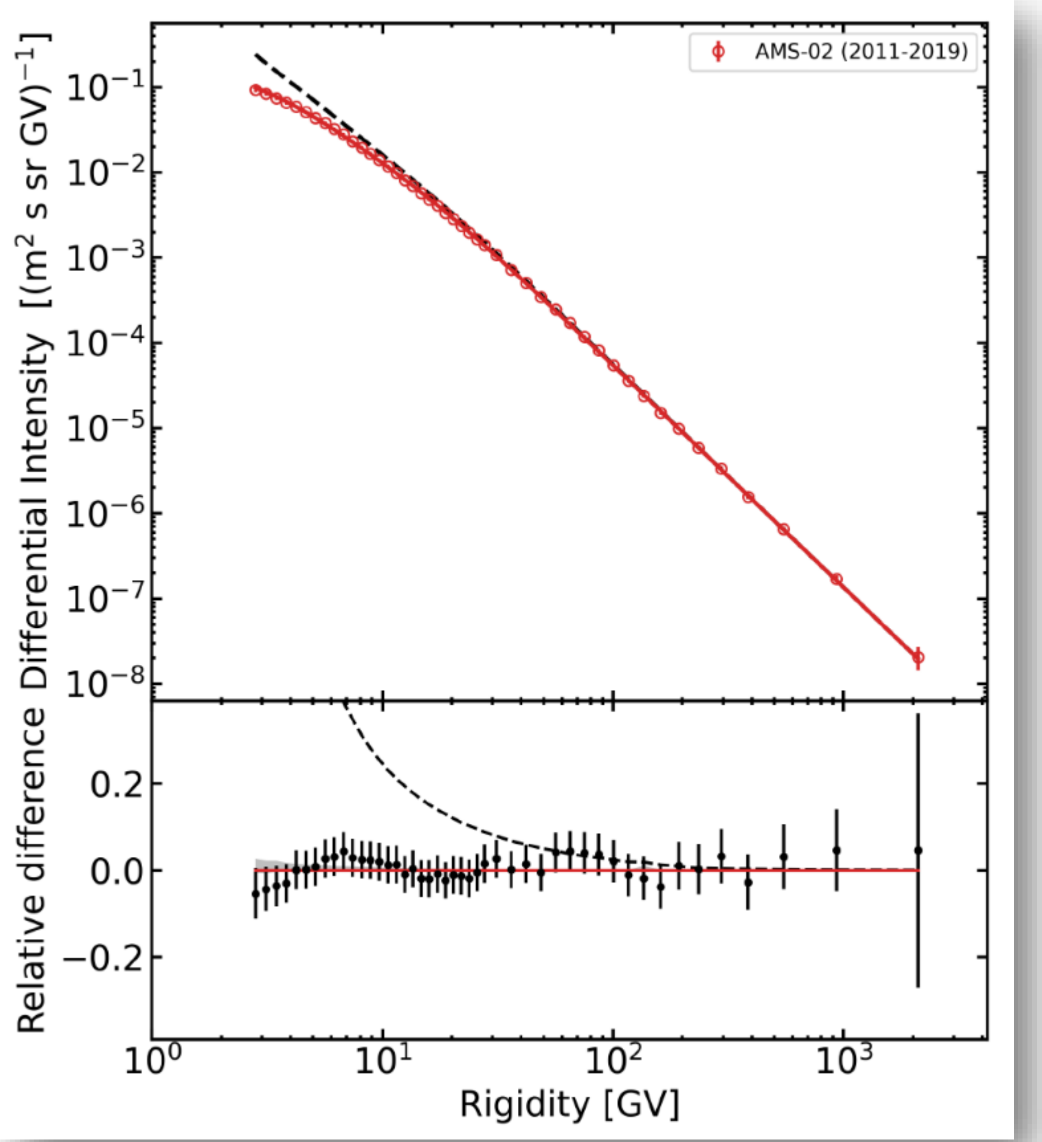

- Most of CR iron at low energies is local and may harbor some features associated with relatively recent supernova activity in the solar neighborhood (Local Bubble).
- The analysis of iron spectrum together with Voyager 1 and ACE-CRIS data reveals an unexpected bump in the iron spectrum and in the Fe/He, Fe/O, and Fe/Si ratios at 1–2 GV, while a similar feature in the spectra of He, O, Si, and in their ratios is absent, hinting at a local source of low-energy CRs.
- The found excess fits well with recent discoveries of radioactive Fe60 deposits in terrestrial and lunar samples, and in CRs.

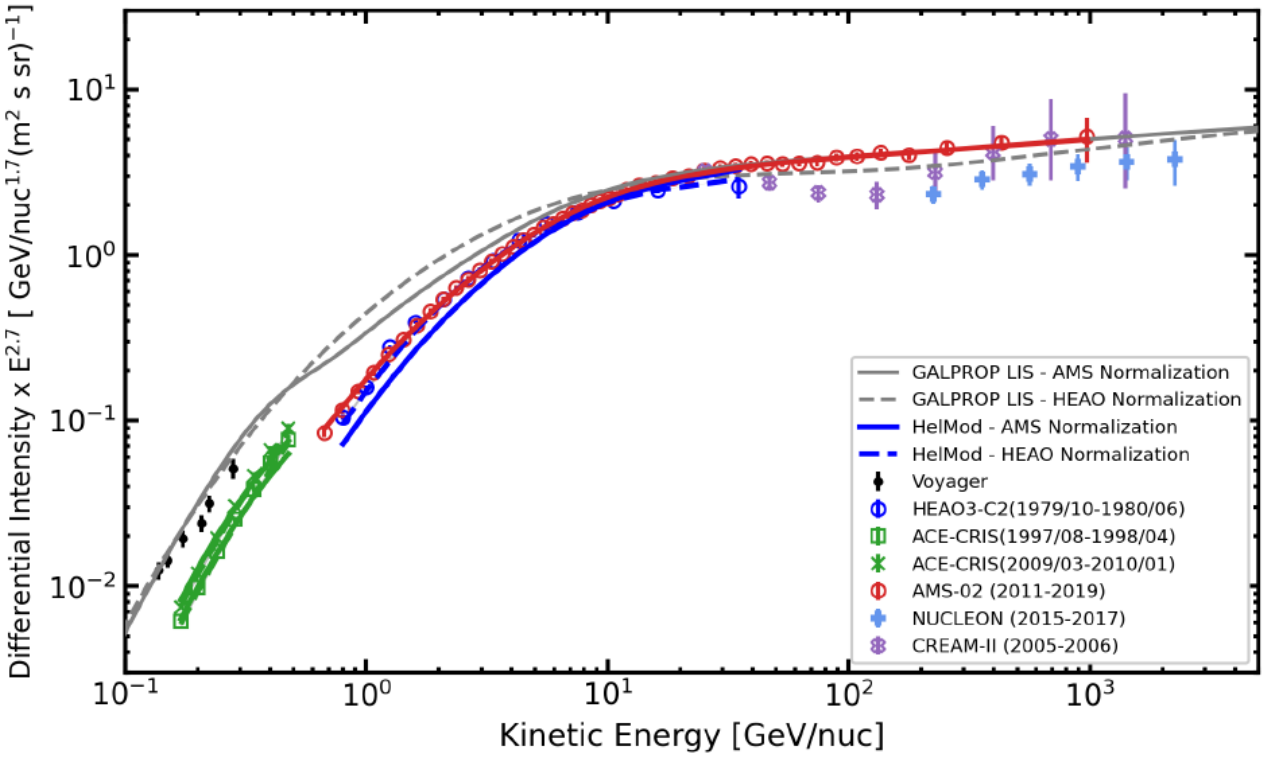

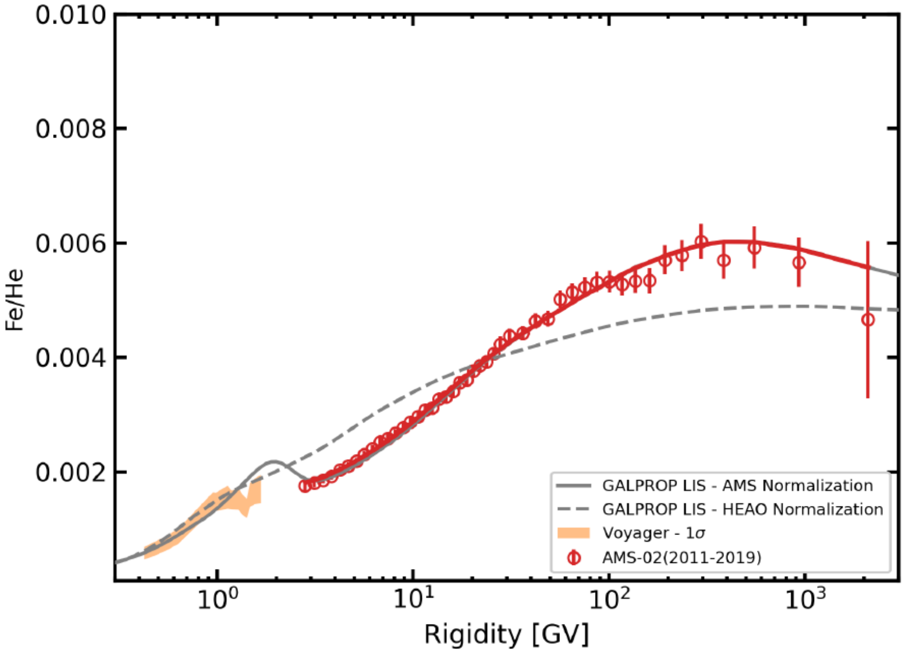

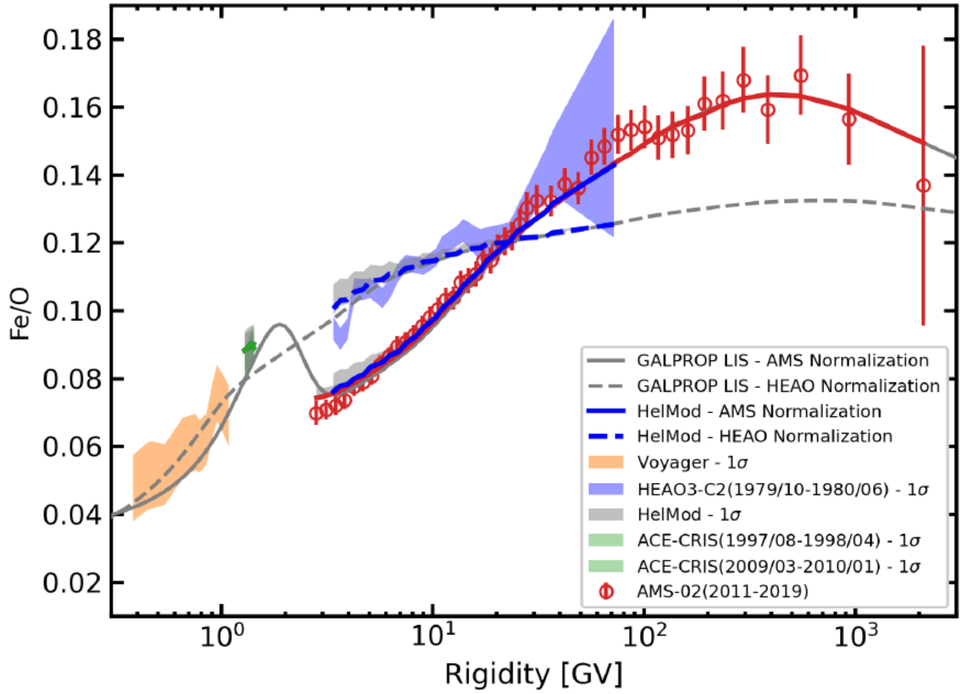

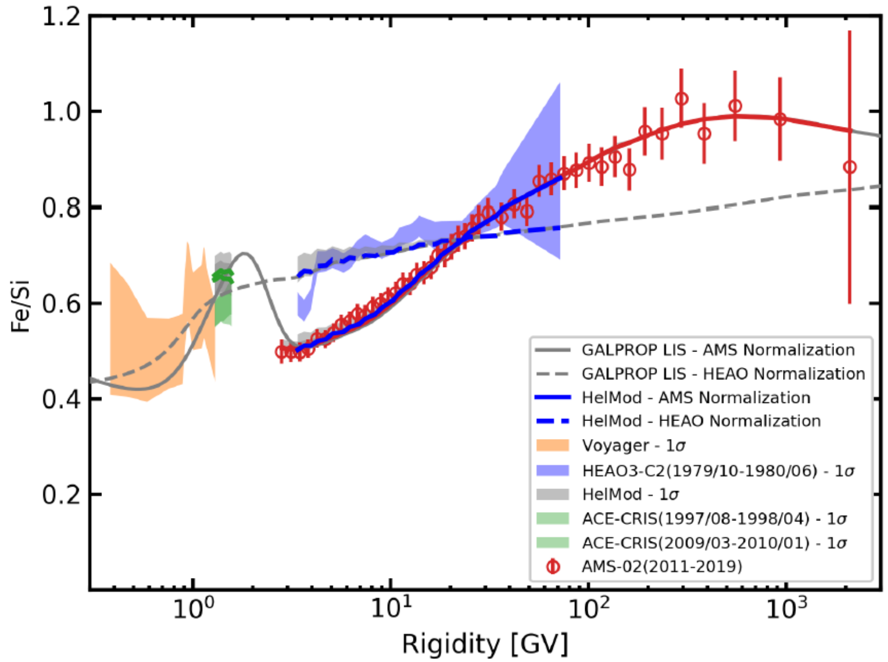

HEAO and AMS-02 data are not compatible for iron, so we had to renormalize Iron to AMS-02: the only way to recover ACE and Voyager-1 data is to introduce a bump in an unknown Fe isotope (Fe60) at the GV scale. Future anomalies in other primary cosmic rays will corroborate this finding

The Propagation Scheme in the Milky Way

$$\underbrace{\frac{\partial\psi}{\partial t}}_{} = \underbrace{q(\vec{r},p)}_{\text{Source}} + \overbrace{\vec{\nabla}\cdot(D_{xx}\vec{\nabla}\psi}^{\text{Diffusion}} \underbrace{- \vec{V}\psi)}_{\text{Convection}} + \overbrace{\frac{\partial}{\partial p}p^2 D_{pp}\frac{\partial}{\partial p}\frac{1}{p^2}\psi}^{\text{Reacceleration}} - \overbrace{\frac{\partial}{\partial p}\left[\dot{p}\psi\right.}^{\text{Energy Loss in ISM}} \underbrace{\left.- \frac{p}{3}(\vec{\nabla}\cdot\vec{V})\psi\right]}_{\text{Adiabatic Expansion}} - \overbrace{\frac{1}{\tau_f}\psi}^{\text{Fragmentation}} - \underbrace{\frac{1}{\tau_r}\psi}_{\text{Decay}}$$

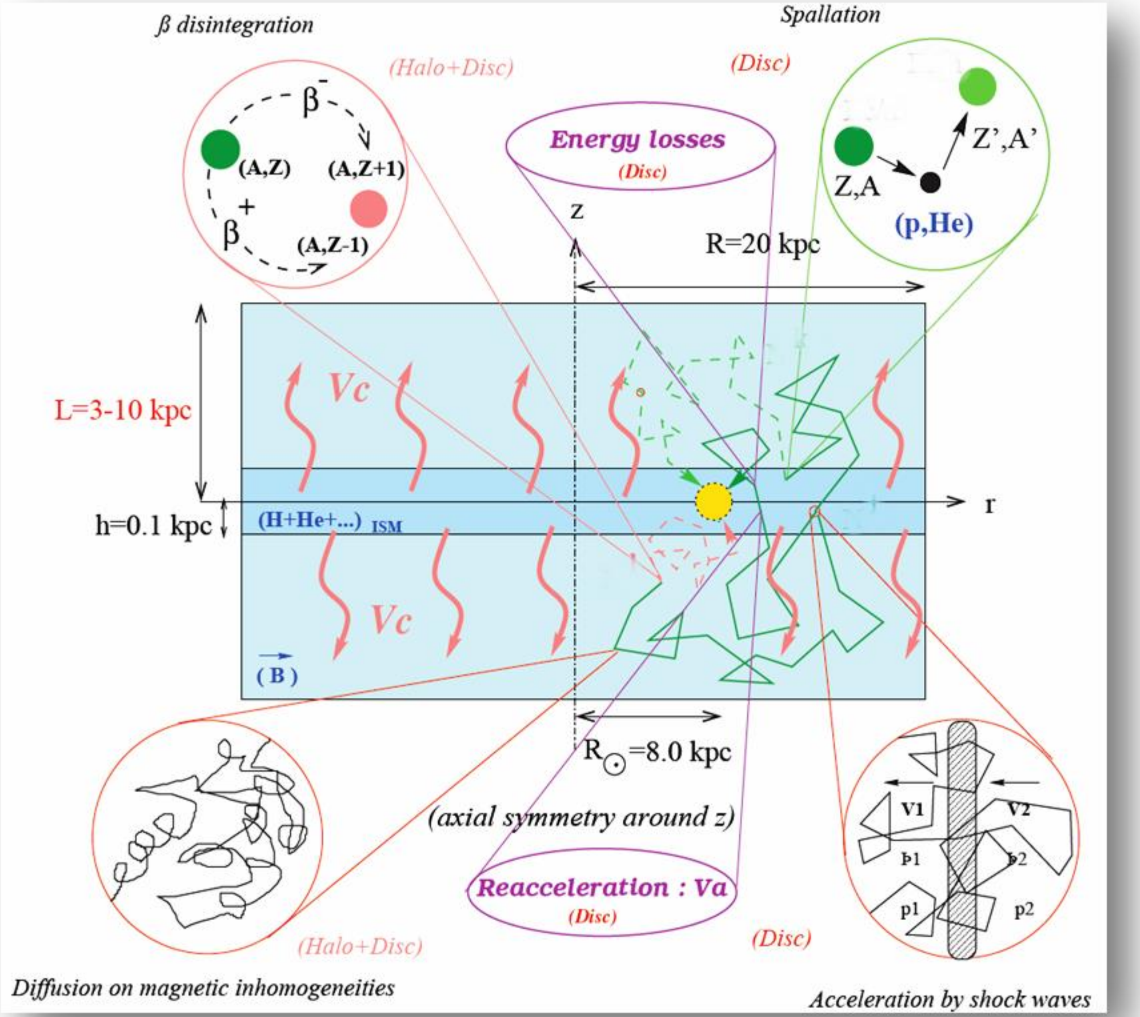

- **Geometry**: halo of thickness z
- **Diffusion**: diffusion in the galactic magnetic field inhomogeneities, propagating through the ISM (D_0, δ)
- **Convection**: galactic wind with velocity gradient dV_c/dz
- **Reacceleration**: interstellar turbulence with Alfvén velocity V_A

5 fundamental parameters space to fix CR propagation